Fırat Üniversitesi Deneysel ve Hesaplamalı Mühendislik Dergisi

FUJECE

DIgSILENT Power Factory Kullanılarak Orta Gerilim Dağıtım Şebekelerinde Güneş Enerji Santrali Entegrasyonunun Etkilerinin Değerlendirilmesi

Merve Ceylan DİLEK[1], Cem HAYDAROĞLU [1*], Heybet KILIÇ[2]

[1]Elektrik Elektronik Mühendisliği Bölümü, Mühendislik Fakültesi, Dicle Üniversitesi, Diyarbakır, Türkiye.
[2]Elektrik ve Enerji Bölümü, Teknik Bilimler Meslek Yüksek Okulu, Dicle Üniversitesi, Diyarbakır, Türkiye.
[1]merve.dilek@dedas.com.tr, [2]cem.haydaroglu@dicle.edu.tr, [3]heybet.kilic@dicle.edu.tr

Geliş Tarihi: 22.03.2025
Kabul Tarihi: 18.07.2025
Düzeltme Tarihi:21.05.2025
doi: https://doi.org/10.62520/fujece.1663319
Araştırma Makalesi

Alıntı: M. C. Dilek, C. Haydaroğlu ve H. Kılıç,''DIgSILENT power factory kullanılarak orta gerilim dağıtım şebekelerinde güneş enerji santrali entegrasyonunun etkilerinin değerlendirilmesi", Fırat Üni. Deny. ve Hes. Müh. Derg., vol. 4, no 3, pp. 524-544, Ekim 2025.

Öz

Günümüzde büyük ölçekli güneş enerji santrallerinin (GES) dağıtım şebekelerine entegrasyonu, gerilim profili, reaktif güç dengesi ve koruma koordinasyonu gibi önemli teknik zorlukları beraberinde getirmektedir. Bu çalışmada, Diyarbakır bölgesinde bulunan pilot bir besleyiciye 1,6 MW ve 16 MW kapasiteli iki GES'in entegrasyonunun şebeke üzerindeki etkileri DIgSILENT Power Factory yazılımı kullanılarak analiz edilmiştir. Gerçek şebeke verileri üzerinden yürütülen senaryo tabanlı analiz kapsamında, yük akışı, gerilim değişimi, ters güç akışı ve kısa devre akımları gibi kritik parametreler detaylı olarak değerlendirilmiştir. Bulgular, artan üretim kapasitelerinin gerilim kararlılığına olumlu katkılar sağladığını ancak koruma sistemlerinde röle ayarları ve kesici kapasiteleri gibi unsurlarda ek düzenlemeler gerektirebileceğini göstermektedir. Çalışma, benzer dağıtım şebekelerinde yenilenebilir enerji entegrasyonu için pratik bir çerçeve sunmakta ve ileride yapılacak detaylı koruma ve kısa devre analizlerine zemin hazırlamaktadır.

Anahtar kelimeler: DIgSILENT power factory, Güneş enerji santrali, Yük akışı analizi, Kısa Devre akımı, Şebeke kararlılığı

*Yazışılan yazar

İntihal Kontrol: Evet – Turnitin
Şikayet: fujece@firat.edu.tr

Firat University Journal of Experimental and Computational Engineering

Evaluation of Solar Power Plant Integration Effects on Medium Voltage Distribution Networks Using DIgSILENT Power Factory

Merve Ceylan DİLEK[1], Cem HAYDAROĞLU[1*], Heybet KILIÇ[2]

[1]Department of Electrical and Electronics Engineering, Faculty of Engineering, Dicle University, Diyarbakir, Türkiye
[2]Department of Electrical and Energy, Technical Sciences Vocational School, Dicle University, Diyarbakir, Türkiye
[1]merve.dilek@dedas.com.tr, [2]cem.haydaroglu@dicle.edu.tr, [3]heybet.kilic@dicle.edu.tr

Received: 22.03.2025
Revision:21.05.2025
Accepted:18.07.2025
doi: https://doi.org/10.62520/fujece.1663319
Research Article

Citation: M. C. Dilek, C. Haydaroğlu and H. Kılıç, "Evaluation of solar power plant integration effects on medium voltage distribution networks using digsilent power factory", Firat Univ. Jour.of Exper. and Comp. Eng., vol. 4, no 3, pp. 524-544, October 2025.

Abstract

The integration of large-scale solar power plants (SPPs) into distribution networks brings significant technical challenges related to voltage profiles, reactive power balance, short-circuit currents, and protection coordination. In this study, the effects of adding two SPPs with capacities of 1.6 MW and 16 MW to a pilot feeder in the Diyarbakır region are analyzed using the DIgSILENT Power Factory software based on real grid data. The scenario-based analysis evaluates critical parameters such as power flow, voltage deviations, reverse power flow, and the expected impact on short-circuit levels. The results show that higher generation capacities contribute positively to voltage stability and load balancing but may require adjustments to relay settings and breaker capacities to maintain protection reliability. This study provides a practical framework for planners and operators considering similar renewable integrations in medium-voltage distribution grids and emphasizes the need for comprehensive protection and fault analyses in future work.

Keywords: DIgSILENT power factory, Solar power plant, Load flow analysis, Short-circuit current, Grid stability

*Corresponding author

1. Introduction

The rapid advancements in technology and the steady growth of the population have led to a concomitant increase in energy demand [1,2]. This energy demand is currently met through the utilization of fossil fuels, which have seen a decline from 82% in 2013 to 80% in 2023 [3]. The transition to renewable energy sources (RES) has gained significant momentum due to mounting environmental concerns and the exhaustion of fossil fuels [4,5]. In response, countries have formulated policies and unveiled support packages to encourage the transition to RESs. According to the Renewables-2024 report published by the International Energy Agency (IEA) in 2024, 5,500 gigawatts (GW) of new renewable energy plants will be commissioned by 2030, with 940 GW commissioned each year if countries continue their current policies [6]. Solar PV and wind account for 95% of these new RES. The IEA Electricity report, published in 2024, indicates that solar PV generation reached 2,000 TWh in 2024, contributing 7% to global electricity generation [7].

In addition to their environmental benefits and unlimited capacity, RESs are subject to certain drawbacks, including their sensitivity to weather conditions, intermittent energy production, and low energy density [8]. RESs have been observed to induce fluctuations and instability in the distribution grid due to their variable generation, which is contingent on weather conditions [9,10]. Solar PV and wind power generation can lead to reverse power flow and power interruptions to the distribution grid due to over- or under-generation [11]. These issues can potentially compromise the quality of electricity in distribution networks [12,13]. Furthermore, the installation of RESs may result in inadequacies in the transmission and distribution infrastructure within the respective regions. To mitigate these challenges, a comprehensive examination of the distribution network infrastructure within the proposed installation site is imperative[14].

The integration of RESs, electric vehicles, and battery systems within the distribution network has precipitated a transformation in the radial distribution network of our nation. In response to this transformation, numerous load flow analysis programs have been developed. These programs are designed to predict the impact of WPPs, electric vehicles, and battery systems on the distribution network and to facilitate informed investment decisions. In [15], the DIgSILENT Power Factory program was utilized to investigate voltage regulation issues that emerged due to the incorporation of solar power plants in the Kahramanmaraş region into the local electricity distribution network. In another study, the DIgSILENT Power Factory program was employed to analyze the load flow changes resulting from the integration of solar PV plants into a real distribution network [16]. Furthermore, the impact of distributed generation facilities on the grid is investigated using the ETAP (Electrical Transient and Analysis Program) program in [17]. In [18], a dynamic analysis of medium voltage (MV) primary electricity distribution network investments with mixed integer programming technique (MIP) was performed using DIgSILENT Power Factory program. The models developed for this analysis were tested in the Mediterranean Electricity Distribution Network region. In [19], a radial network model was created in Digsilent Power Factory program. The presence of a faulty line in the network model, accompanied by a series capacitor, was detected through the implementation of the k-ERC classification method. In [20], an IEEE 13-bus test system was developed in the DIgSILENT Power Factory program and analyzed for the location of harmonic loads. In [21], the DIgSILENT Power Factory program was utilized to conduct a comprehensive analysis of the region where the establishment of an electric vehicle charging station is planned. In [22], the PSS/E program was utilized to investigate the current status of the electricity networks in the Çanakkale region, and a detailed analysis was carried out for the transition to renewable energy systems. In [23] the DIgSILENT Power Factory program was employed to model the transmission lines in the Ankara region, accompanied by a thorough protection analysis. In [24], the IEEE 14 bus-bar test system was modeled using the DIgSILENT Power Factory program. The maximum load levels that this bus-bar system can reach are analyzed in detail by considering the parameters affecting the stability. In [25], the locations of electric vehicle charging stations in Kırıkkale province were determined by employing the Monte-Carlo algorithm. Subsequently, a comprehensive analysis was conducted for the identified locations in the DIgSILENT Power Factory program. In [26], a model for residential areas was developed in MATLAB/Simulink, and the integration of electric vehicles into the Turkish low voltage distribution networks was investigated. In [27], DIgSILENT Power Factory was

modeled using real data from Kocaeli University Umuttepe Campus. Subsequently, a comprehensive analysis was conducted on the grid ethics of electric vehicles. In [28], the impact of wind and solar power plants on the grid is analyzed in detail for the pilot region using the DIgSILENT Power Factory program.

In this study, the effects on the grid of adding a 1.6 MW and 16 MW solar power plant to a pilot feeder in the Diyarbakır region are analyzed in detail using the DIgSILENT Power Factoryprogram.

2. Material and Method

2.1. Diyarbakır electricity distribution network

The city of Diyarbakır is situated within the Dicledaş region and has amassed a subscriber base that exceeds 400,000 individuals. The map obtained as a result of the load flow analysis performed on the electricity network in the Diyarbakır region using DIgSILENT Power Factory software reveals the voltage profiles and load conditions of the network's nodes. The DIgSILENT Power Factory model of the Diyarbakır electricity distribution network is presented in Figure 1. The shapes and colors of the symbols employed in the map are classified according to the voltage levels and loading rates of the relevant nodes. Consequently, the points displayed in shades of green and blue signify that voltage levels are within acceptable limits and loadings are within normal parameters. In contrast, orange and red colors indicate voltage drops, overloading, or potential critical areas. Sections of the network that were inactive or disconnected during the analysis are represented by gray points. The results of the analysis indicate that, while the network structure is predominantly stable and balanced on a regional scale, there are critical points in terms of voltage and loading in specific locations. These findings necessitate network improvement and reinforcement in these areas.

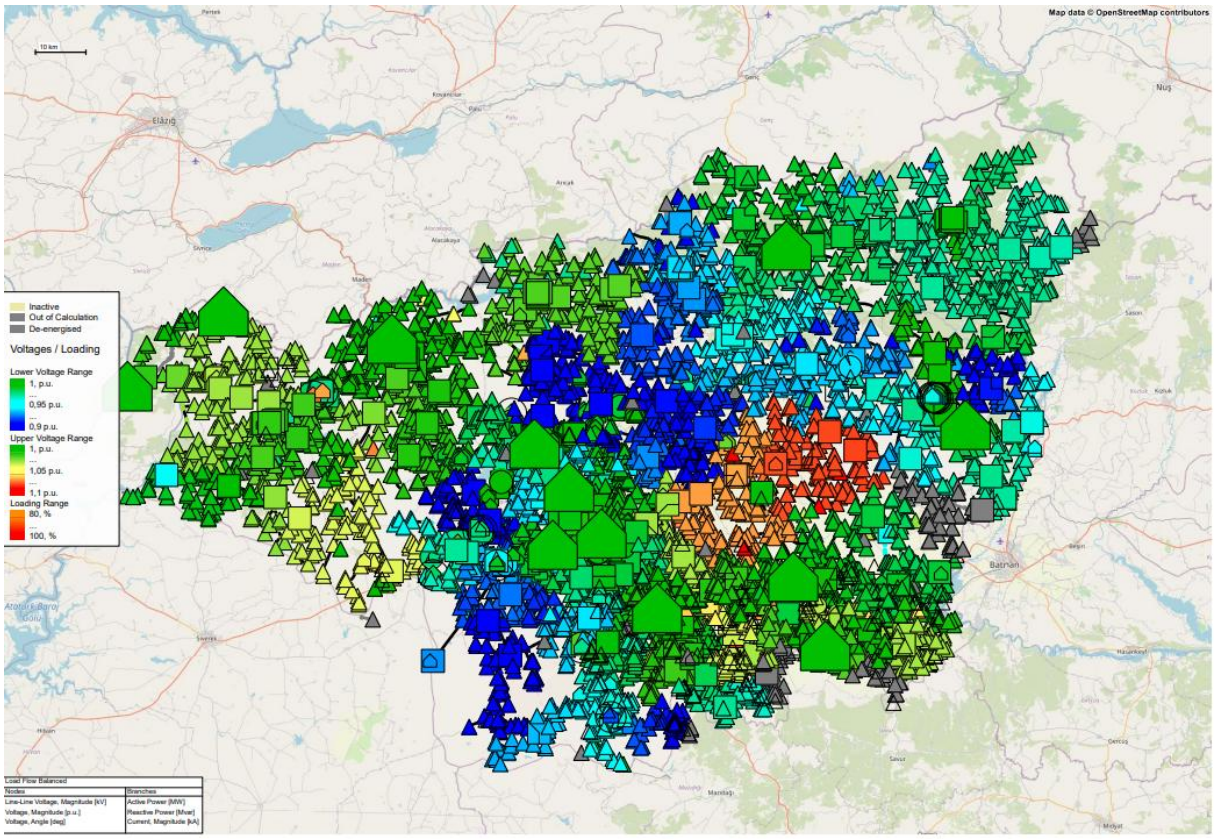

Figure 1. Diyarbakır electricity distribution network

2.2. DIgSILENT power factory

Power Factory (DIgSILENT) is a comprehensive software suite developed for the analysis, simulation, and optimization of electric power systems. This software is widely used by engineers and researchers in academia and industry. It boasts a robust toolset, enabling users to comprehensively understand, analyze, and enhance the intricate designs of electrical power systems [29]. Power Factory's versatility extends to its applications in both academic research and industrial settings, making it a valuable asset in these domains. Specifically, the software provides a high-precision simulation environment for power flow analysis, short circuit calculations, harmonic analysis, dynamic stability assessments, and integration of renewable energy systems. Power flow analysis is employed to assess voltage profiles and power distribution within power systems, while short circuit analysis is imperative for determining system reliability and the appropriate protection settings. Additionally, harmonic analysis is employed to identify potential harmonic distortions, thereby enhancing power quality [30].

Power Factory's modular structure affords its users a flexible working environment, providing a system adaptable to different types of analysis. The data management module facilitates detailed modeling of power grid components, while the single line diagram interface enables graphical representation of grid elements. The calculation engine facilitates the execution of complex calculations, including power flow, short circuit, and dynamic analysis, with optimal efficiency and precision [31].

Power Factory is a software that offers automation and programming support to its users, thereby enhancing the efficiency of their analysis processes. This enhancement is facilitated by the integration of Python and the DIgSILENT Programming Language (DPL), which enables the automation of analyses and the acceleration of repetitive processes. Furthermore, Python API support facilitates seamless integration with external databases, thereby streamlining data analysis and reporting processes, a crucial aspect for large-scale data management [32].

Power Factory boasts high accuracy and calculation methods that comply with international standards, including IEC and IEEE. This enables reliable analysis and optimization of energy systems. Notably, it provides detailed modeling options for the integration of renewable energy sources, facilitating the assessment of solar and wind energy systems' integration into the grid. In conclusion, Power Factory (DIgSILENT) is an indispensable analysis and simulation tool for electrical engineers and a powerful software that provides comprehensive and accurate results in power systems studies. It is the ideal solution for users who want to perform reliable analysis in both academic research and industrial projects [33].

3. Results

In this study, an examination of the Diyarbakır electricity distribution network was conducted. Two separate Solar Power Plants (SPPs) with an installed capacity of 1.6 MW and 16 MW were added to a sample feeder as depicted in Figure 2. The TM F13 was determined to be a suitable candidate for connection to the aforementioned sample feeder.

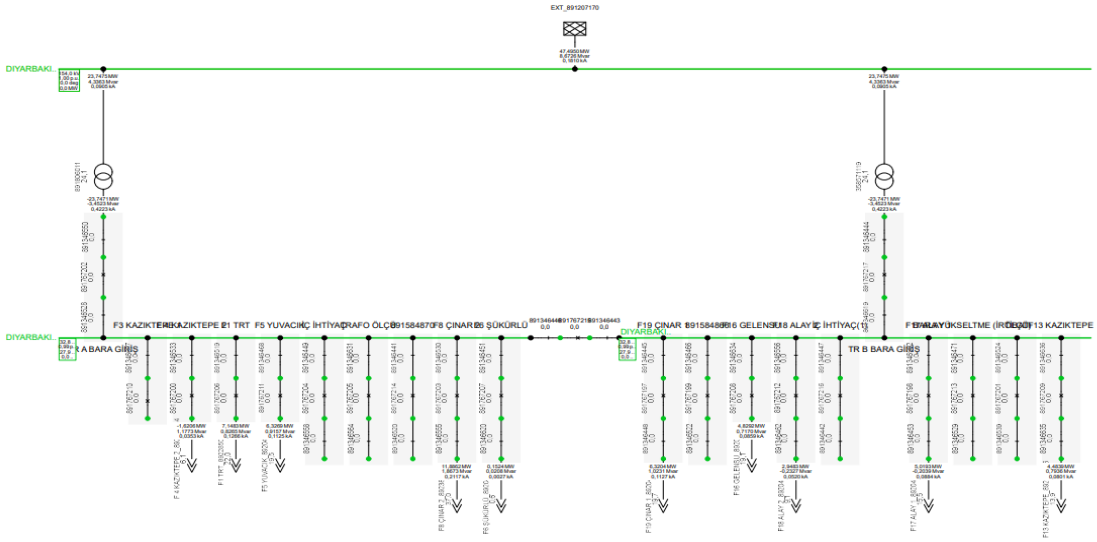

Figure 2. Sample TM feeder single line diagram and load status without SPP connection

An analysis of the load flow of Sample TM without SPP integration in Figure 2 reveals that the system is generally stable, with the voltage level at the 154 kV bus-bar reaching an ideal level of 1.00 p.u. The Sample feeder contributes the most significant load, with 47.49 MW of active power and 8.67 MVAR of reactive power. The distribution of load on other feeders is homogeneous, with lower levels. The Şükürlü line exhibits negative active power (-1.62 MW) and positive reactive power (1.18 MVAR), suggesting the presence of a local power supply or interaction with a distinct substation. The system's current state can be characterized as stable. However, the integration of SPPs or additional power sources, particularly in high-load areas such as Sample, will contribute to load balancing on the TM and enhance grid performance.

Table 1. Sample 1 TM Load case (without SPP connected)

Starting Point	Target Point	Current (kA)	Reactive Power (MVAR)	Active Power (MW)
Sample TM	TR A Bus-bar Entry	0.1810 kA	8.6726 MVAR	47.4950 MW
TR A Bus-bar Entry	Sample	0.0801 kA	0.7936 MVAR	4.4839 MW
Sample	TR B Bus-bar Entry	0.0884 kA	-0.2039 MVAR	5.0193 MW
TR B Bus-bar Entry	Çınar 1	0.0905 kA	4.3363 MVAR	23.7475 MW
Çınar 1	TR B Bus-bar Entry	0.4223 kA	-3.4523 MVAR	-23.7471 MW
TR B Bara Girişi	Çınar 2	0.0520 kA	-0.2327 MVAR	2.9483 MW
Çınar 2	Alay 1	0.0859 kA	0.7170 MVAR	4.8292 MW
Alay 1	Alay 2	0.1127 kA	1.0231 MVAR	6.3204 MW
Alay 2	Yuvacık	0.0027 kA	0.0208 MVAR	0.1524 MW
Yuvacık	Şükürlü	0.2117 kA	1.8673 MVAR	11.8862 MW
Şükürlü	Çınar 1	0.1125 kA	0.9157 MVAR	6.3269 MW
Çınar 1	Çınar 2	0.1266 kA	0.8265 MVAR	7.1483 MW
Çınar 2	TR A Bus-bar Entry	0.0353 kA	1.1773 MVAR	-1.6206 MW

As illustrated in Table 1, the Sample TM is currently operating at 154 kV and has a structure with different load distribution. The maximum power consumption, recorded at 47.495 MW, is observed in the Sample 1 TM to the TRA A bus-bar entrance. In contrast, an active power flow of -1.6206 MW is noted in the opposite direction from Çınar 2 to the TRA A bus-bar entrance. The reactive power flow remains predominantly at

low levels, with the highest recorded value of 8.6726 MVAR observed on the Sample 1 TM line. The lines are predominantly characterized by active consumption, however, the Şükürlü line exhibits negative active power flow (-1.6206 MW) and positive reactive power flow (1.1773 MVAR), suggesting that this line is supplied by power generation or alternative sources. While the TM generally maintains balance, it is crucial to consider the load density along specific lines when assessing system performance.

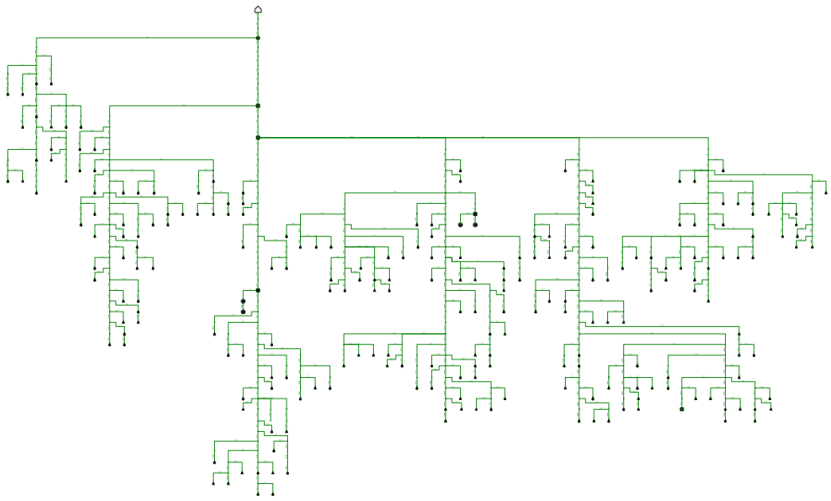

Figure 3. Sample 1 TM Hierarchical Single Line Diagram

Upon examination of the single line diagram of the aforementioned feeder, TM F13 (see Figure 3), it is evident that the load distribution on the feeder is predominantly balanced, albeit with minimal density. The current values along the line are predominantly at low levels, ranging from 0.1 to 2.2 kA. The presence of numerous branch points in the diagram suggests that the energy distribution exhibits a homogeneous structure. However, it is observed that the current and power values exhibit higher variability at specific points along the line compared to other regions, suggesting variations in consumption density across these areas. The conclusion drawn from this analysis suggests that, while the existing network structure is stable, localized high loads along the line should be taken into consideration during network planning. In the context of future planning, it would be advantageous to explore the potential of augmenting the Sample feeder with an additional power supply or the integration of a solar power plant.

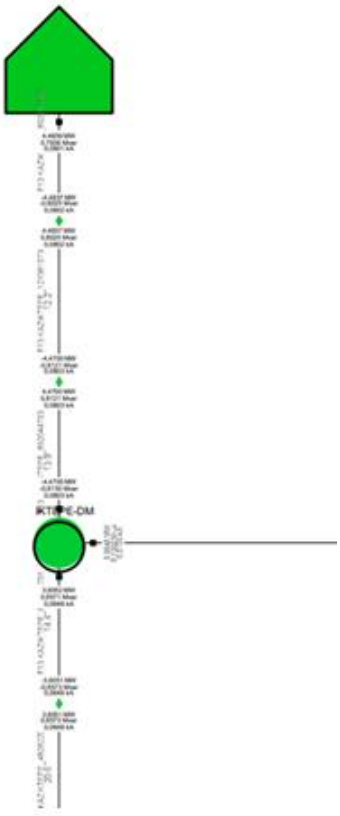

Figure 4. Sample 1 TM F13 Sample feeder load flow hierarchical single line image without SPP connected

When the current load flow status of the Sample 1 TM F13 Sample feeder in Figure 4 is examined, it is seen that the line realizes bidirectional power flow. There is a total flow of approximately 4.4839 MW of active power and 0.8025 MVAR of reactive power from the Sample TM to the Sample distribution center. On the other hand, approximately -4.4700 MW active power and -0.8121 MVAR reactive power flows in the opposite direction from Sample DM to Diyarbakır TM. This situation reveals that the feeder in question has a bidirectional energy flow and shows a bidirectional operation in terms of energy generation or consumption depending on local conditions. Although the Sample feeder is generally balanced, the integration of additional energy sources in the region or increasing the line capacity should be considered for load demands that may increase in the future.

Table 2. Sample TM F13 Sample grid power values without SPP connection

Starting Point	Target Point	Current (kA)	Reactive Power (MVAR)	Active Power (MW)
Sample TM_F13 Sample	Sample -DM	0.0803 kA	-0.8130 MVAR	-4.4700 MW
Sample TM	Sample	0.0803 kA	0.8121 MVAR	4.4700 MW
Sample	Line Area	0.0802 kA	0.8025 MVAR	4.4837 MW
Line Area	Sample	0.0803 kA	-0.8121 MVAR	-4.4700 MW
Sample	Main Grid	0.0648 kA	0.6573 MVAR	3.6051 MW
Main Grid	Sample	0.0648 kA	-0.6586 MVAR	-3.6008 MW
Sample	Line Area	0.0648 kA	0.6571 MVAR	3.6052 MW
Line Area	Sample	0.0648 kA	-0.6573 MVAR	-3.6051 MW
Sample	Main Grid	0.0801 kA	0.7936 MVAR	4.4839 MW
Main Grid	Sample	0.0802 kA	-0.8025 MVAR	-4.4837 MW

As illustrated in Table 2, a bidirectional power flow is observed between Sample TM and Sample distribution center. While 4.4700 MW of active power and 0.8130 MVAR of reactive power are observed to flow from Diyarbakır TM to Sample distribution center (sample-DM), 3.6051 MW of active power and 0.6573 MVAR of reactive power are seen to flow in the opposite direction (from sample to Grid Zone). The alteration in the signs of the active and reactive powers signifies that the region in question is engaged in the exchange of energy with the generation source or disparate connection points, in addition to power consumption. The power flows between the line zone and the grid zone exhibit analogous values, and a stable situation is observed in terms of power balance. This observation suggests that augmenting the line capacity or integrating local generation sources could be advantageous in meeting future energy demands.

3.1. Sample TM 1.6 MW SPP addition case

The integration of a 1.6 MW SPP into the specified TM model has been shown to exert a favorable influence on the prevailing load flow and energy equilibrium. The integration of the SPP results in a reduction of the active power demand on the TM, attributable to the provision of local generation capacity. A quantitative analysis of the grid structure reveals that the SPP connection provides approximately 2.8897 MW of active power and 0.8644 MVAR of reactive power to the TM. This reduction in load, resulting from the SPP's integration, leads to a favorable impact on the energy balance. The current values are recorded at approximately 0.0533 kA, indicating a stable and balanced system load distribution. However, the reactive power values are negative, indicating the need for careful management of the reactive power balance of the system at this level. In conclusion, the incorporation of the 1.6 MW SPP into the specified TM model has a beneficial effect on the security of energy supply and contributes to the alleviation of the grid load.

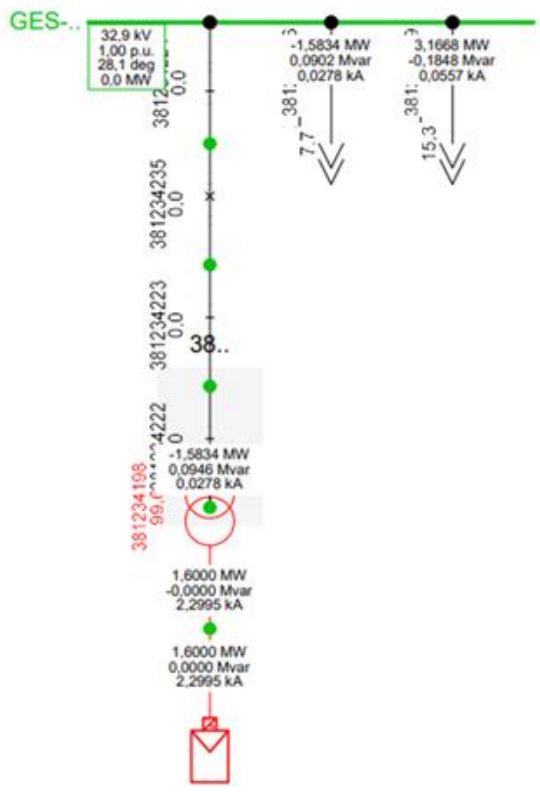

Figure 5. 1.6 MW SPP Single line and load flow diagram

As illustrated in Figure 5, the specified SPP represents a renewable energy generation facility with an installed capacity of 1.6 MW. Presently, 1.6 MW of active power is being generated from this SPP, while the reactive power generation remains at a null value. At the point of system connection, the voltage level is 32.9 kV (1.00 p.u.), and the current value is measured at 2.2995 kA. The plant exhibits

bidirectional energy flow, supplying 1.5834 MW of power to the system and drawing approximately 0.09 MVAR of reactive power in return. The stability of the power balance and voltage level in the system is evident, and the incorporation of the SPP into the grid is expected to play a substantial role in enhancing the regional energy supply and meeting load demands.

Table 3. 1.6 MW SPP Power ratings

Parameter	**SPP**	**Feeder**	**TM**
Power (MW)	1.6	-2.8897	-2.8897
Voltage (kV)	32.9		
Current (kA)	2.2995	0.0533	0.0533
Reactive Power (MVAR)	0.0902	-0.8654	-0.8654
Phase Angle (deg)	28.1		

As indicated by the data presented in Table 3, the 1.6 MW SPP plant functions at an operating voltage of 32.9 kV and a current level of 2.2995 kA. This results in the provision of 1.6 MW of active power and 0.0902 MVAR of reactive power to the grid. However, the energy flow in the feeder and TM direction is negative, with active power values of -2.8897 MW and reactive power values of -0.8654 MVAR. These findings indicate that the SPP generation is insufficient to meet the current consumption, and the line is still drawing energy from the grid. Despite the presence of a balanced load flow with a low current of 0.0533 kA, the direction of power flow and the reactive power situation indicate that this level of SPP is inadequate to meet the total load on the TM. However, it contributes to alleviating the load.

3.2. Sample TM 1.6 MW SPP impact on feeder

The single line diagram in the figure shows the energy flow following the connection of a 1.6 MW SPP between the sample TM and the sample Distribution Center (sample-DM). Approximately 2.8958 MW of active power and 0.8280 MVAR of reactive power are provided along the line towards the sample TM, and the current value is approximately 0.0530 kA. It can be seen that the direction of energy flow is from Sample-DM to Diyarbakır TM and that the Sample-DM point has shifted to the energy generating position. This situation contributes to a more balanced and efficient operation of the grid by reducing the load demand on the TM. In addition, the balanced power flow on the line shows that the SPP connection has positive effects on grid stability.

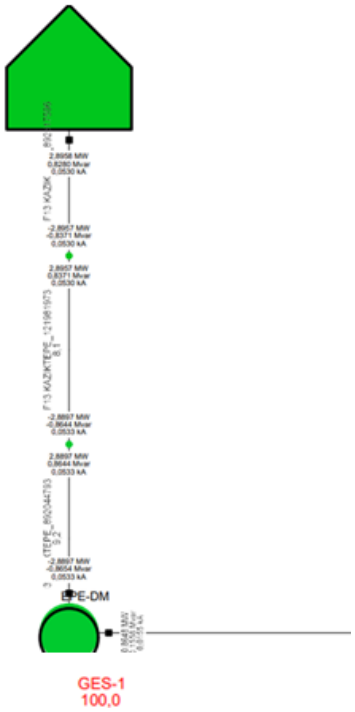

Figure 6. Impact of 1.6 MW SPP on feeder and Load Flow

As illustrated in Figure 6, the energy flow following the connection of a 1.6 MW SPP between the sample TM and the sample Distribution Center (Sample-DM) is depicted in a single line diagram. The line supplies approximately 2.8958 MW of active power and 0.8280 MVAR of reactive power towards Diyarbakır TM, with a current value of approximately 0.0530 kA. It is evident that the direction of energy flow is from the sample-DM to the Diyarbakır TM, thereby transforming the sample-DM point into an energy producer. This phenomenon contributes to a more balanced and efficient operation of the grid by reducing the load demand on the TM. Furthermore, the balanced power flow along the line indicates that the SPP connection exerts a favorable influence on grid stability.

Table 4. Effect of SPP on the feeder and Load Flow Values

Region	Current	Reactive Power	Active Power
Sample-DM	0.0533 kA	-0.8654 MVAR	-2.8897 MW
SampleTM	0.0533 kA	0.8644 MVAR	2.8897 MW
Line Area	0.0530 kA	0.8371 MVAR	2.8957 MW
Sample	0.0533 kA	-0.8644 MVAR	-2.8897 MW
Transformer Area	0.0530 kA	0.8280 MVAR	2.8958 MW
Grid Connection	0.0530 kA	-0.8371 MVAR	-2.8957 MW

As illustrated in Table 4, the integration of the 1.6 MW SPP results in a net power flow within the grid. The sample TM and Line Zone exhibit positive active power values of 2.8897 MW and 2.8957 MW, respectively, and reactive power generation of 0.8644 and 0.8371 MVAR. In contrast, the sample DM and the sample zone are in the consumer position, exhibiting -2.8897 MW active power and -0.8654 MVAR reactive power. The transformer zone functions as an energy producer, generating 2.8958 MW of active power and 0.8280 MVAR of reactive power, which is then supplied to the grid. The current values, estimated at approximately 0.0533 kA, are indicative of a balanced system load flow. This observation indicates that the incorporation of 1.6 MW SPP has exerted a favorable influence on energy management, thereby modifying the regional energy balance.

3.3. Sample TM 1.6 MW SPP impact on substation (TM) load flow

As illustrated in Figure 7, the single line diagram demonstrates the grid condition subsequent to the integration of a SPP with a capacity of 1.6 MW into the sample TM. The diagram reveals that sample TM is fed through two distinct transformer inputs (TRA and TRB bus-bar inputs) and subsequently distributed to various regions, including sample, Çınar, Gelensu, Alay, Şükürlü, and Yuvacık. Following the establishment of the SPP connection, a notable shift in energy flow direction was observed, particularly within the sample feeder. This alteration resulted in the initiation of energy supply to sample TM with a power output of approximately 2.89 MW, directed via sample-DM. This development has had a favorable impact on the grid's performance and stability, achieved by reducing the load on sample TM through the incorporation of SPP. The balanced voltage and power distribution within the system further substantiates the positive impact of the 1.6 MW SPP integration on regional energy management.

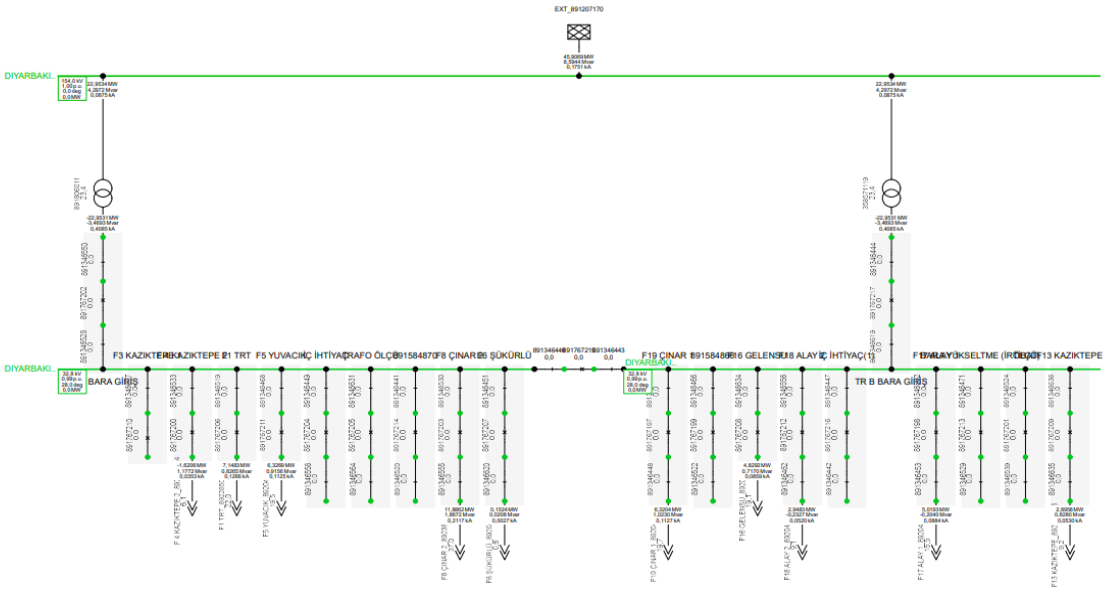

Figure 7. 1.6 MW SPP impacts on TM and Load Flow Operated Single Line Schematic

As illustrated in Table 5, the configuration of the load distribution and the power flow dynamics within the system underwent alterations subsequent to the incorporation of the 1.6 MW capacity SPP in the designated TM. The sample 1 TM exhibits the highest load, with an active power of 45.9069 MW and a reactive power of 8.5944 MVAR. Conversely, the Grid Connection draws power from the system, exhibiting a negative power flow of -22.9531 MW. The load values in areas such as Çınar, Alay and Şükürlü are moderate, while the Yuvacık area provides energy with negative active power (-1.6206 MW) or exchanges energy bidirectionally with the system. The collective current levels are found to be within acceptable ranges, exhibiting stability. However, this state of affairs underscores the necessity for meticulous oversight with respect to grid operation, particularly in the context of bidirectional power flows, where effective energy balance management is paramount.

Table 5. Sample TM 1.6 MW SPP Impact on Substation (TM) Load Flow

Region	Current	Reactive Power	Active Power
Sample TM	0.1751 kA	8.5944 MVAR	45.9069 MW
Sample	0.0530 kA	0.8280 MVAR	2.8958 MW
Line Area	0.0884 kA	-0.2040 MVAR	5.0193 MW
Çınar 1	0.0875 kA	4.2972 MVAR	22.9534 MW
Grid Connection	0.4085 kA	-3.4693 MVAR	-22.9531 MW
Şükürlü	0.2117 kA	1.8672 MVAR	11.8862 MW
Alay 2	0.1125 kA	0.9156 MVAR	6.3269 MW
Çınar 2	0.1266 kA	0.8265 MVAR	7.1483 MW
Yuvacık	0.0353 kA	1.1772 MVAR	-1.6206 MW

3.4. Sample TM 16 MW SPP addition case

The integration of the 16 MW SPP into the specified TM has resulted in substantial alterations to the energy flow within the grid, leading to significant relief in the load distribution on the TM and its associated feeders. The SPP, when connected to the system, generates 16 MW of active power, thereby providing a substantial amount of energy to the sample TM. This, in turn, enables the TM to transition from a state of energy reception to one of energy generation. This development has led to an enhancement in the security of energy supply within the region and a reduction in the load on the system. However, as the voltage level (37.8 kV - 1.14 p.u.) and current value (20,1909 kA) increased, regular monitoring of the voltage and reactive power balance of the grid became imperative. The high-capacity SPP integration, in sum, plays a pivotal role in meeting the energy demands of the region, thereby promoting effective energy management and grid stability.

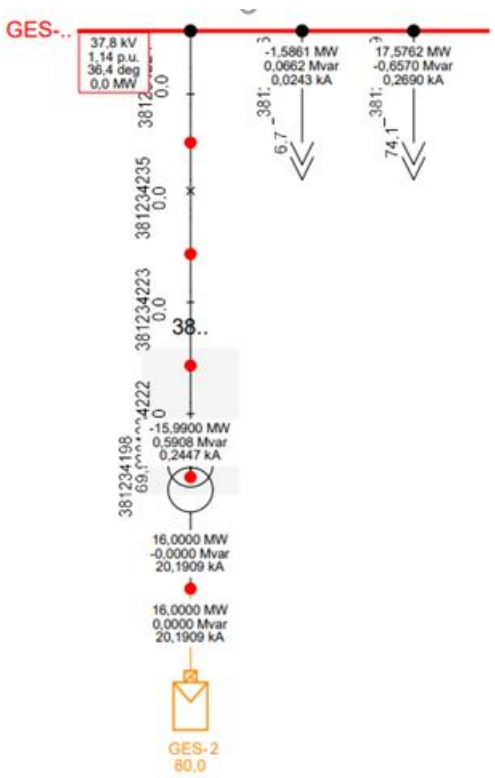

Figure 8. 16 MW SPP Single Line diagram and Load flow

As illustrated in Figure 8, the single line diagram demonstrates the power flow subsequent to the integration of the 16 MW GES-2 into the system. The diagram reveals that SPP-2 generates 16 MW of active power and supplies energy to the grid with a current of approximately 20.1909 kA. Consequently, a net flow of 15.990 MW of active power and 0.5908 MVAR of reactive power is observed, indicating a backflow towards consumption at the point of connection. The grid voltage increased to 37.8 kV (1.14 p.u.), and the phase angle registered at 36.4 degrees. These observations indicate that the integration of SPP-2 modifies the direction of energy flow within the system by facilitating high power generation. Furthermore, it enhances system stability by positively impacting the load balance of the line. However, it is imperative to note that the high voltage level necessitates stringent monitoring of the grid to ensure effective voltage regulation.

Table 6. 16 MW SPP Load Flow Values

Parameter	**SPP**	**Feeder**	**TM**
Power (MW)	16	9.3363	9.3363
Voltage (kV)	37.8		
Current (kA)	20.1909	0.1712	0.1712
Reactive Power (MVAR)	0.0662	-2.7482	-2.7482
Phase Angle (deg)	36.4		

As indicated by the values presented in Table 6, the integration of the SPP, with a capacity of 16 MW, into the TM model results in the generation of 16 MW of active power at a voltage of 37.8 kV and a current level of 20.1909 kA. This development has enabled the system to become energy generating, with an active power output of approximately 9.3363 MW and a reactive power flow of -2.7482 MVAR in the direction of the TM and feeder. The observation of negative reactive power suggests that the line is consuming reactive power, necessitating close monitoring of the system's reactive power management. The phase angle, measured at 36.4 degrees, further validates the direction of energy flow from the SPP to the TM. The integration of high-power SPPs has been demonstrated to reduce the load on the Sample TM, strengthen the energy supply, and enhance system stability.

3.5. Feeder impact of sample TM 16 MW SPP

The integration of a 16 MW SPP into the Sample TM has resulted in a substantial alteration within the feeder. Prior to the integration of the SPP, the feeder functioned as a consumer; however, subsequent to the connection of the 16 MW SPP, it transitioned into a state of energy production. The analysis revealed a net flow of 9.3363 MW of active power and -2.7482 MVAR of reactive power through the feeder to the TM, indicating a transition from a consumer to a producer role. This shift contributed to the fulfillment of regional energy demands and the alleviation of capacity constraints on power transmission lines through a reduction in load ratios. However, the presence of negative reactive power necessitates measures to ensure grid stability and effective reactive power management. Consequently, the feeder has assumed a pivotal role in regional power management by reversing the direction of energy flow.

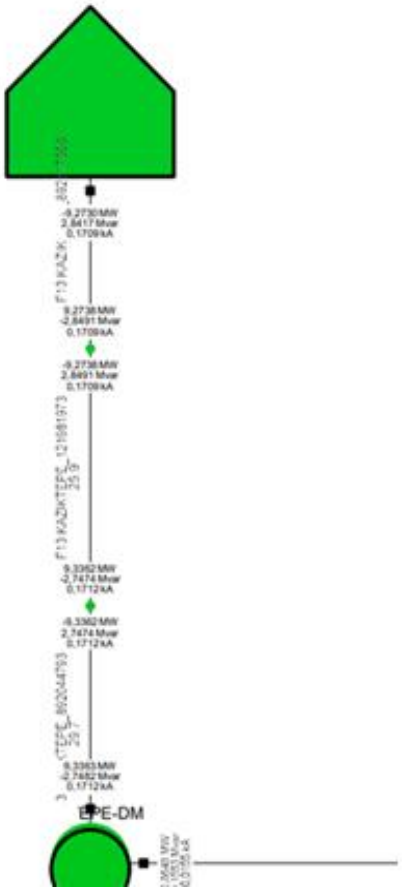

Figure 9. Feeder impact of 16 MW SPP

As illustrated in Figure 9, the energy flow through the Sample DM feeder following the connection of a 16 MW SPP to the Sample TM reveals a notable shift in power flow dynamics. Subsequent to the integration of the SPP, an estimated 9.3363 MW of active power and 2.7482 MVAR of reactive power were observed to flow from the sample DM to the Diyarbakır TM. This high power resulted in an increase in the current level through the feeder to 0.1712 kA, indicating a shift from the feeder's previous consumer position to its new role as an energy producer. Consequently, energy transmission was achieved towards the sample TM. While this change offers certain benefits, such as enhanced grid security and reduced line load, it also necessitates close monitoring of the feeder's capacity and reactive power management due to the rise in current and reactive power values.

Table 7. Feeder impact of 16 MW SPP

Region	Current	Reactive Power	Active Power
Sample-DM	0.1712 kA	-2.7482 MVAR	9.3363 MW
SampleTM	0.1712 kA	2.7474 MVAR	-9.3362 MW
Line Area	0.1709 kA	2.8491 MVAR	-9.2738 MW
Sample	0.1712 kA	-2.7474 MVAR	9.3362 MW
Transformer Area	0.1851 kA	2.5931 MVAR	-10.2011 MW
Grid Connection	0.1709 kA	-2.8491 MVAR	9.2738 MW

As illustrated in Table 7, the power flow in the regions underwent substantial alterations subsequent to the 16 MW SPP connection. The Sample-DM and Sample zones are identified as energy producers, with an active power output of 9.3363 MW and a negative reactive power of -2.7482 MVAR. In contrast, the Sample TM zone is designated as an energy consumer, exhibiting an active power consumption of -

9.3362 MW. The Line Zone and the Grid Connection Zone exhibited comparable power values; however, their operational directions were antithetical. The Transformer Zone demonstrated the highest level of consumption, with an active power consumption of 10.2011 MW. The current values were found to be predominantly balanced at approximately 0.17-0.18 kA, and the system maintained stability. Nevertheless, owing to the presence of substantial power variations and reactive power imbalances, it is imperative to undertake continuous monitoring of the system and execute requisite adjustments.

3.6. Impact of sample TM 16 MW SPP on substation (TM) load flow

The incorporation of a 16 MW SPP into the aforementioned TM has resulted in substantial alterations to the grid's power flow direction and load balance. The integration of a SPP of this magnitude has effectively transformed the DG from a consumer to an energy producer, thereby contributing to the region's energy supply. The active power flowing through the TM has been recorded at approximately 9.3363 MW, leading to an increase in the current level to 0.1712 kA. Concurrently, the reactive power values have exhibited a negative trend, underscoring the necessity for enhanced reactive power management within the system.This development has led to several notable outcomes. Firstly, it has bolstered the energy supply security of the region. Secondly, it has facilitated the distribution of load, thereby enhancing grid stability. However, it is imperative to maintain constant vigilance and intervene as necessary in order to ensure the effective control of high voltage and reactive power.

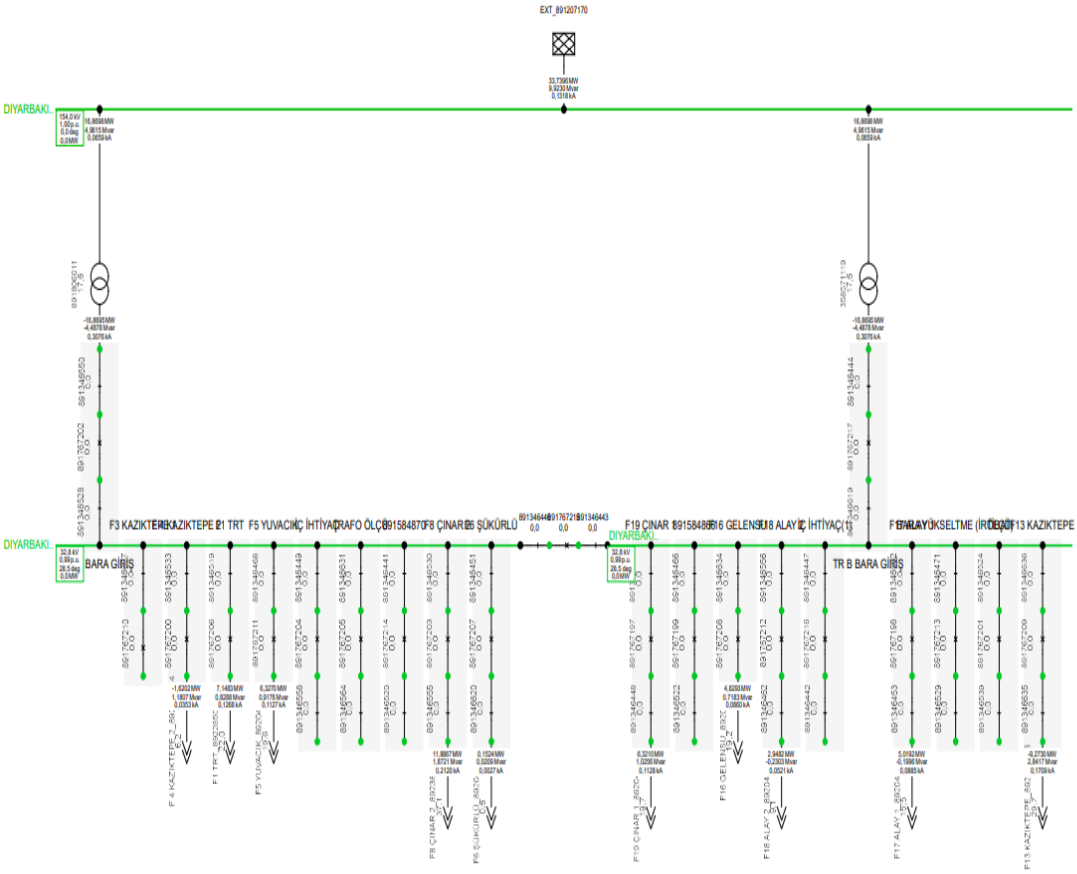

Figure 10. 16 MW SPP impacts on TM and Load Flow Operated Single Line Schematic

As illustrated in Figure 10, the single line diagram of the specified TM model demonstrates the power flow and load distribution subsequent to the incorporation of the 16 MW SPP into the system. The model

substation receives energy from two distinct transformer inputs (TRA and TRB bus-bars) and subsequently supplies energy to regions such as Yuvacık, Şükürlü, Çınar, Alay and Gelensu through multiple feeders. Following the integration of the 16 MW SPP, the direction of energy flow undergoes a reversal, with energy being transferred toward the TM through the sample area and connected lines. This transformation of the TM from an energy consumer to an energy producer has a beneficial effect on the power distribution of the region. Despite the stability of the overall power balance and currents in the system, reactive power management and continuous monitoring of voltage levels are necessary due to the presence of bidirectional power flow.

Tablo 8. Impact of 16 MW SPP on TM

Region	**Current**	**Reactive Power**	**Active Power**
Sample TM	0.1318 kA	9.9230 MVAR	33.7396 MW
Sample	0.1709 kA	2.8417 MVAR	-9.2730 MW
Line Area	0.0885 kA	-0.1996 MVAR	5.0192 MW
Çınar 1	0.0659 kA	4.9615 MVAR	16.8698 MW
Grid Connection	0.3076 kA	-4.4878 MVAR	-16.8695 MW
Şükürlü	0.2120 kA	1.8721 MVAR	11.8867 MW
Alay 2	0.1127 kA	0.9176 MVAR	6.3270 MW
Çınar 2	0.1268 kA	0.8288 MVAR	7.1483 MW
Yuvacık	0.0353 kA	1.1807 MVAR	-1.6202 MW

As indicated by the data presented in Table 8, substantial alterations have been observed in the regional load flows following the incorporation of a 16 MW capacity SPP into the Sample TM. It is noteworthy that Sample 1 TM maintains its position as the region with the highest power consumption, exhibiting an active power of 33.7396 MW and a reactive power of 9.9230 MVAR. It is also observed that the Grid Connection and Sample regions continue to draw power from the system, albeit with negative active power values. Çınar 1, Şükürlü, Alay 2, and Çınar 2 regions demonstrate moderate active and reactive power values. Notably, the Yuvacık region exhibits a reverse flow of -1.6202 MW power, indicating local energy exchange.While the energy flow within the system remains balanced, alterations in power flow direction have emerged due to the incorporation of high-capacity SPPs. This integration has contributed to the reduction of the load on the TM and increased the security of energy supply. However, it is imperative to maintain continuous monitoring and control of the reactive power balance to ensure grid stability.

This study analyzes the impact of 1.6 MW and 16 MW SPP additions on the electrical grid. The results demonstrate that these additions lead to observable changes in active power, feeder current level, substation current level, phase angle, power factor, and power levels. The present study undertakes a thorough examination of the load flow outcomes of 1.6 MW and 16 MW capacity SPPs integrated within the grid, with a specific focus on the impact of two distinct power levels on the electricity system. The analytical framework encompasses a comprehensive evaluation of key parameters such as voltage, current, reactive power, phase angle, and power factor, derived from the detailed load flow calculations. The critical values of the load flow analysis for 1.6 MW and 16 MW capacity SPPs over single line schemes are enumerated in Table 9 below, as per the data obtained from DIgSILENT Power Factory

Table 9. Load Flow Analysis of 1.6 MW and 16 MW SPPs

Parameter	1.6 MW SPP	16 MW SPP
Voltage (kV)	32.9	37.8
Current (kA)	2.2995	20.1909
Reactive Power (MVAR)	0.0902	0.0662
Phase Angle (°)	28.1	36.4
Power Factor	0.999	0.996

An analysis of the impacts of 1.6 MW and 16 MW SPPs on the electricity grid, as presented in Table 9, reveals alterations in various parameters. For the 1.6 MW SPP, the feeder current is calculated as 0.0533 kA, and the substation current is calculated as 0.0533 kA. For the 16 MW SPP, the feeder current increases to 0.1712 kA, and the substation current increases to 0.1712 kA. In terms of reactive power, the feeder reactive power and substation reactive power for 1.6 MW SPP are -0.8654 MVAR and -0.8654 MVAR, respectively, while these values are -2.7482 MVAR for 16 MW SPP. The integration of the 16 MW SPP into the grid resulted in an increase in voltage from 32.9 kV to 37.8 kV, thereby demonstrating the positive impact of large-scale SPPs on the voltage profile of the grid.The phase angle was measured at 28.1° for the 1.6 MW SPP and 36.4° for the 16 MW SPP. This rise in phase angle indicates that reactive power requirements escalate at higher power levels. As SPPs typically generate low levels of reactive power, it can be inferred that large-capacity plants may necessitate reactive power compensation. The power factor for both plants approaches 1, with values of 0.999 for the 1.6 MW SPP and 0.996 for the 16 MW SPP. The findings indicate that the system functions efficiently in terms of active power generation and supplies power to the grid with minimal harmonics and losses. The commissioning of the 16 MW SPP results in substantial current and reactive power fluctuations on feeders and substations. These results underscore the critical role of appropriate transformer capacity and reactive power management strategies in large-scale SPP projects.

4. Conclusions

This study comprehensively investigated the effects of integrating two solar SPPs with capacities of 1.6 MW and 16 MW into a real distribution feeder in the Diyarbakır region, using DIgSILENT Power Factory. The scenario-based analysis was conducted with actual operational data, providing practical insights into how increased distributed generation impacts voltage profiles, reactive power flow, reverse power flow, and short-circuit currents within a medium-voltage network. A pronounced escalation in current values is observed when the SPP is augmented from 1.6 MW to 16 MW. For instance, the current on the Sample-DM line has been shown to increase from 0.0533 kA to 0.1712 kA. This observation indicates an increase in the system's load capacity and a corresponding rise in the current drawn by the transmission lines. Furthermore, substantial changes in active power flow are evident. At a SPP of 1.6 MW, the power flow on the Sample-DM line was -2.8897 MW, while at a SPP of 16 MW, this value increased to 9.3363 MW. A similar trend is observed in the active power in the Sample 1 TM area, which has shown a significant change from 2.8897 MW to -9.3362 MW. These observations indicate that a larger capacity SPP has a substantial impact on the power supply of the line.

The augmentation of the SPP capacity elicited substantial alterations in the reactive power values. In the Sample-DM region, the reactive power exhibited a decline from -0.8654 MVAR to -2.7482 MVAR. The negative reactive power increase signifies an augmented inductive load within the system, necessitating a power factor correction. This scenario underscores the requirement for enhanced capacitive compensation within the system. In the Sample 1 TM zone, the reactive power exhibited an increase from 0.8644 MVAR to 2.7474 MVAR, while the current value in the transformer zone increased from 0.0530 kA to 0.1851 kA. This suggests that the transformer is experiencing a higher current load, which may indicate an increase in the level of loading. To avert such scenarios, meticulous analysis of load distribution is imperative, along with the strategic augmentation of transformer capacity when the need arises. A notable shift in active power is also observed at grid connections, with a notable increase from -2.8957 MW to 9.2738 MW, accompanied by a 16 MW SPP. This underscores the possibility of overloading at specific grid points, necessitating proactive measures to ensure grid stability and reliability.

The results demonstrate that higher capacity SPPs significantly improve voltage stability and help balance feeder loading by supplying local generation; however, they also pose potential challenges such as reverse power flow and variations in short-circuit current levels that may require protection scheme adjustments. It was noted that inverter-based SPPs contribute limited fault current compared to conventional synchronous generators, which can influence the sensitivity and selectivity of existing relays and breakers.

In light of these findings, this study highlights the importance of performing detailed protection coordination and short-circuit analyses before commissioning similar renewable integration projects. The practical

framework and methodological approach presented here can be adapted for other regions with similar network structures, supporting planners and operators in making informed decisions for future grid expansion.

For future work, it is recommended to extend the analysis by incorporating advanced reactive power compensation devices (e.g., STATCOM, SVC) and smart grid controls to mitigate voltage fluctuations and ensure reliable protection coordination under various operating scenarios. Additionally, investigating the combined impact of larger SPPs and emerging loads such as electric vehicles could provide further valuable insights for distribution network planning.

5. Acknowledgment

I would like to thank Dicle Elektrik Dağıtım AŞ and DIgSILENT Power Factory Turkey family for their support for this study.

6. Author Contribution Declaration

The authors contributed equally to the article.

7. Ethics Committee Approval and Conflict of Interest

“There is no conflict of interest with any person/institution in the prepared article”

8. Ethics Committee Approval and Conflict of Interest Declaration

No artificial intelligence-based tools or applications were used in the preparation of this study. There is no need to obtain ethics committee permission for the article prepared. There is no conflict of interest with any person/institution in the article prepared.

9. References

[1] H. A. Abd el-Ghany, I. A. Soliman, and A. E. ELGebaly, "An advanced wide-area fault detection and location technique for transmission lines considering optimal phasor measurement units allocation," Alex. Eng. J., vol. 61, no. 5, pp. 3971–3984, 2022.
[2] E. Kavuş Demir, C. Haydaroğlu, H. Kılıç, M. Çelikpençe, and M. M. Şahin, "IoT-driven monitoring and optimization of hybrid energy storage systems with supercapacitors in distribution networks," Turk. J. Electr. Power Energy Syst., vol. 5, no. 2, pp. 86–95, Jun. 2025.
[3] IEA, "World energy outlook 2024," Paris, 2024.
[4] C. Haydaroğlu, H. Kılıç, and B. Gümüş, "Performance analysis and comparison of performance ratio of solar power plant," Turk. J. Electr. Power Energy Syst., vol. 4, no. 3, pp. 190–199, Oct. 2024.
[5] S. Shahzad, T. R. Alsenani, O. Alrumayh, A. Altamimi, and H. Kilic, "Adaptive hydrogen buffering for enhanced flexibility in constrained transmission grids with integrated renewable energy system," Int. J. Hydrogen Energy, vol. 144, no. Feb., pp. 637–651, 2025.
[6] IEA, "Renewables 2022: analysis and forecast to 2027," [Online]. Available: https://www.iea.org/reports/renewables-2022. [Accessed: 2022].
[7] IEA, "Electricity 2025," 2025.
[8] P. Saenger, N. Devillers, K. Deschinkel, M.-C. Pera, R. Couturier, and F. Gustin, "Optimization of electrical energy storage system sizing for an accurate energy management in an aircraft," IEEE Trans. Veh. Technol., vol. 66, no. 7, pp. 5572–5583, Jul. 2017.
[9] N. Narasimhulu, M. Awasthy, R. Pérez de Prado, P. B. Divakarachari, and N. Himabindu, "Analysis and impacts of grid integrated photo-voltaic and electric vehicle on power quality issues," Energies, vol. 16, no. 2, 2023.
[10] İ. Türk, H. Kılıç, C. Haydaroğlu, and A. Top, "Robust load frequency control in hybrid microgrids using type-3 fuzzy logic under stochastic variations," Symmetry, vol. 17, no. 6, p. 853, May 2025.
[11] M. Thakur, A. Patil, and G. Patil, "The current state of the art for PV grid connected system issues with power quality," in Proc. Int. Interdiscip. Humanitarian Conf. Sustain. (IIHC), 2022, pp. 1515–1520.
[12] A. Mazza et al., "Interaction among multiple electric vehicle chargers: Measurements on harmonics and power quality issues," Energies, vol. 16, no. 20, pp. 1–17, 2023.
[13] M. Türk, C. Haydaroğlu, and H. Kılıç, "Machine learning-based detection of non-technical losses in power distribution networks," Firat Univ. J. Exp. Comput. Eng., vol. 4, no. 1, pp. 192–205, Feb. 2025.
[14] S. Shahzad, T. R. Alsenani, A. N. Alrumayh, A. Almutairi, and H. Kilic, "Fault ride-through capability improvement in hydrogen energy-based distributed generators using STATCOM and deep-Q learning," Int. J. Hydrogen Energy, vol. 143, no. Oct., pp. 1000–1012, 2024.
[15] F.A. Fırış, and M. Şekeli, "Güneş enerji santrallerinin şebeke gerilimine etkilerinin incelenmesi; Kahramanmaraş örneği," Kahramanmaraş Sütçü İmam Univ. Mühendislik Bilimleri Derg., vol. 24, no. 2, pp. 53–65, Jun. 2021.
[16] Z. Aygün, F. A. Fırış, and M. Şekkeli, "Güneş enerji santrallerinin şebeke entegrasyonunda yük akışı analizlerinin incelenmesi: Kahramanmaraş örneği," Kahramanmaraş Sütçü İmam Univ. Mühendislik Bilimleri Derg., vol. 26, no. 2, pp. 331–345, Jun. 2023.
[17] Z. Baş, A. İncesu, and A. S. Yılmaz, "Investigating the effects of local power plants on the stability of distribution networks," Kahramanmaraş Sütçü İmam Univ. Mühendislik Bilimleri Derg., vol. 20, no. 2, pp. 97–104, Aug. 2017.
[18] O. B. Tör, M. E. Cebeci, M. Koç, and A. N. Güven, "Dynamic optimization of long term primary electric distribution network investments based on planning metrics," J. Fac. Eng. Archit. Gazi Univ., vol. 33, no. 1, pp. 227–237, 2018.
[19] D. C. Samuk, and F. M. Nuroğlu, "A new wide area-based algorithm to determine faulted line in series-compensated grid using k-nearest neighbor (k-NN) classification method," J. Fac. Eng. Archit. Gazi Univ., vol. 36, no. 2, pp. 871–882, 2021.
[20] F. Özel, N. Yörükeren, and İ. G. Tekdemir, "Total harmonic power method for harmonic source detection in distribution system," J. Fac. Eng. Archit. Gazi Univ., vol. 39, no. 1, pp. 359–370, 2023.

[21] D. Yıldızhan, A. K. Erenoğlu, and O. Erdinç, "Elektrikli araç entegrasyonunun dağıtım sistemine etkilerinin incelenmesi ve şarj istasyonu altyapısının tayin edilmesi," Mühendislik Bilimleri ve Tasarım Derg., vol. 10, no. 4, pp. 1232–1242, Dec. 2022.
[22] Y. Özgören, and S. Koyuncu, "Geleceğin teknolojisi yenilenebilir enerji sistemlerine geçişte Çanakkale yöresi elektrik şebekelerinin mevcut durumu ve optimizasyonu," Çanakkale Onsekiz Mart Univ. Fen Bilimleri Enstitüsü Derg., vol. 4, no. 2, pp. 212–236, Dec. 2018.
[23] M. Saygılı, and S. S. Tezcan, "Ankara bölgesi için enerji iletim hattı koruma modellemesi analizi ve uygulaması," Gazi Univ. Fen Bilimleri Derg. Part C: Tasarım ve Teknoloji, vol. 7, no. 2, pp. 303–316, 2019.
[24] U. Fesli, M.B. Özdemir, and Ş. Özdemir, "IEEE 14 bara sistemine bağlanabilecek maksimum yük seviyelerinin belirlenmesi," Gazi Univ. Fen Bilimleri Derg. Part C: Tasarım ve Teknoloji, vol. 11, no. 1, pp. 111–132, Mar. 2023.
[25] M. Kiliçarslan Ouach, and E. Çam, "Investigation on the electrical vehicles effects on the electrical power grid," El-Cezeri J. Sci. Eng., vol. 8, no. 1, pp. 21–35, 2021.
[26] R.B. Mert, and N. Umurkan, "Konut bölgelerinde elektrikli taşıt şarj istasyonlarının elektrik şebekesine entegrasyonunun analizi," Karadeniz Fen Bilimleri Derg., vol. 13, no. 3, pp. 965–980, Sep. 2023.
[27] A.T. Yapıcı, and N. Abut, "Elektrikli araç şarj istasyonu konum tasarımında, Digsilent yazılımı kullanılarak Kocaeli Üniversitesi Umuttepe Kampüsü için sample uygulama," Black Sea J. Eng. Sci., vol. 7, no. 5, pp. 1066–1080, Sep. 2024.
[28] K. Dinçer, and M. Dursun, "Elektrik dağıtım şebekelerinde rüzgar ve güneş enerji santrallerinin şebeke entegrasyonunun Digsilent'ta esnek AC iletim sistemleri (FACTS) ile incelenmesi," Düzce Univ. Teknik Bilimler Derg., vol. 2, no. 2, pp. 26–46, Dec. 2024.
[29] Z. Deng, G. Todeschini, K. L. Koo, and M. Mulimakwenda, "Modelling renewable energy sources for harmonic assessments in digsilent Power Factory: Comparison of different approaches," in Proc. 11th Int. Conf. Simulation Modeling Methodologies, Technologies and Applications (SIMULTECH), 2021, pp. 130–140.
[30] C. H. Lin, "A power dispatch approach to enhance dynamic stability for incorporating a large scale PV farm into an isolated grid," IET Renew. Power Gener., vol. 19, no. 1, pp. 1–18, Jan. 2025.
[31] O. G. Carmona, K. M. Silva, V. M. V. Marín, D. A. G. Neira, and C. C. M. Cano, "A novel approach for reconfiguring large-scale power distribution systems using genetic algorithms and DIgSILENT Power Factory," in Proc. 3rd Int. Conf. Electr., Comput., Commun. Mechatronics Eng. (ICECCME), 2023, pp. 1–6.
[32] Y. Dai, M. Panteli, and R. Preece, "Python scripting for DIgSILENT Power Factory: Enhancing dynamic modelling of cascading failures," in Proc. IEEE Madrid PowerTech, 2021, pp. 1–6.
[33] V. Vergara, and J. D. Pinzón, "Automation of power system security assessment using Python and DIgSILENT Power Factory," in Proc. IEEE PES GTD Latin America Conf. Ind. Expo. (GTDLA), 2024, pp. 1–6.